Z. Kristallogr. Suppl. **26** (2007) 429-434

Utilizing total scattering to study the Jahn-Teller transition in $La_{1-x}Ca_xMnO_3$

E. S. Božin[1,*], X. Qiu[1], R. J. Worhatch[1], G. Paglia[1], M. Schmidt[2], P. G. Radaelli[2], J. F. Mitchell[3], T. Chatterji[4], Th. Proffen[5], and S. J. L. Billinge[1]

[1]Department of Physics and Astronomy, Michigan State University, East Lansing, MI 48824-2320, USA
[2]ISIS, CCLRC Rutherford Appleton Laboratory, Chilton-Didcot, OX11 0QX, Oxfordshire, United Kingdom
[3]Material Science Division, Argonne National Laboratory, Argonne, IL 60439, USA
[4]Institute Laue-Langevin, Boîte Postale 156, 38042 Grenoble Cedex 9, France
[5]Lujan Neutron Scattering Center, Los Alamos National Laboratory, Los Alamos, NM 87545, USA
[*] Contact author; e-mail: bozin@pa.msu.edu

Keywords: total scattering, atomic pair distribution function, CMR manganites

Abstract. Total scattering based atomic pair distribution function (PDF) analysis, with the advent of high data throughput neutron powder diffractometers, helps understanding the nature of the Jahn-Teller (JT) phase transition in $La_{1-x}Ca_xMnO_3$ colossal magnetoresistive (CMR) manganites. The JT distortion of the MnO_6 octahedra, is long-range ordered in the orthorhombic (O) phase, but disappears in the pseudo-cubic (O') phase crystallographically. An anomalous unit cell volume contraction occurs at the transition. The PDF study indicates that the distortion persists *locally* deep in the O' phase, contrary to the crystallographic view. Simultaneously, local structural features observed in PDF at 10.3 Å, sensitive to the oxygen sublattice changes, evolve dramatically across the transition. The same effect is observed irrespective of the way the O-O' phase boundary is crossed: it is seen both in the temperature series data for x=0, and in the doping series data at 310 K and at 550 K.

Introduction

The hole-doped $La_{1-x}Ca_xMnO_3$ (LCMO) series have been the subject of significant interest for decades due to the complex interplay between the spin, charge, orbital and lattice degrees of freedom [1-6]. The parent $LaMnO_3$ (LMO) has an A-type antiferromagnetic ground state, with long-range ordered JT distorted MnO_6 octahedra, exhibiting four shorter (~1.94 Å) and two longer (~2.17 Å) Mn-O bonds, and has orthorhombic (O) symmetry (s.g. *Pbnm*) [7, 8]. When heated above T_{JT}~750 K, the structure becomes pseudo-cubic (O'), but the system retains the same space group [9]. At this JT-transition a loss of long-range orbital order is

observed, and the JT-distortions disappear crystallographically. The temperature of the O-O' transition abruptly lowers with Ca doping, and it becomes as low as 35 K at x=0.2 [9]. Although the insulating pseudo-cubic phase is of great importance, as it hosts the ferromagnetism and CMR effect, its exact nature is still not fully understood [10-13]. The JT-transition is argued to be order-disorder in character [12, 14], but the exact mechanism is still debated [15-17]. The local JT distortion in the undoped endmember, as recently shown, remains with full magnitude all the way up to the highest temperature and the rhombohedral phase [15]. The same study suggested that the ground-state-like orbital order remains within clusters ~16 Å in diameter above the T_{JT}. The nature of the O-O' transition appears to have the same origin when the phase line is crossed both vs temperature at fixed doping, and vs doping at fixed temperature [18]. Here we extend these results to the case when the phase line is crossed as a function of doping at 550 K temperature, deep in the insulating phase. The results agree with these obtained for 310 K. Using the same set of data crystallographic results are further obtained for the evolution of the unit cell volume with doping at 550 K. Anomalous volume contraction is observed upon crossing into the pseudo-cubic O' phase along the doping axis, in agreement with earlier T-dependent studies at fixed doping [14, 16].

Experimental

The local structural information is obtained by the real-space atomic pair distribution function (PDF) analysis of the neutron diffraction data collected at NPDF diffractometer at LANSCE, and at GEM diffractometer at ISIS. The temperature dependence of the x=0 sample was carried out at 14 temperatures from 300 K up to 1150 K at NPDF. At the same instrument data were collected for 13 samples spanning $0 \le x \le 0.5$ doping range at 550 K. The data at 310 K for the same doping range were collected at GEM. Sample preparation and the measurement details including data processing methodology are specified elsewhere [15, 19, 20]. The experimental PDF, G(r), is obtained through a sine Fourier transform of the total scattering structure function, S(Q), where Q is the momentum transfer, via

$$G(r) = \frac{2}{\pi}\int_0^\infty F(Q)\sin(Qr)dQ\,, \qquad (1)$$

using the program PDFGETN [21]. The radial distribution function (RDF), R(r), is related to G(r) through a series of simple arithmetic operations [20]. Both functions are peaked at distances separating pairs of atoms. We show here PDFs that were obtained using high resolution total scattering data up to a very high value of momentum transfer, Q_{MAX}=35Å^{-1}. The full profile refinements of experimental PDFs is obtained using the modelling program PDFFIT [22], while the Rietveld refinements on the diffraction patterns of the same data is carried out using the program GSAS [23, 24] to obtain the crystallographic values.

Results

The data presented here are a subset of an extensive set of data collected at high throughput neutron diffraction instruments to accurately evaluate local structural properties across the phase diagram of LCMO [19]. The advent of modern synchrotron based high flux sources allows for new, previously undetected structural details to emerge. Figure 1 shows detailed

phase diagram of LCMO as mapped out by the O2 isotropic crystallographic displacement parameter. The ridge centred at around x=0.175 at low T tracks the O-O' phase boundary.

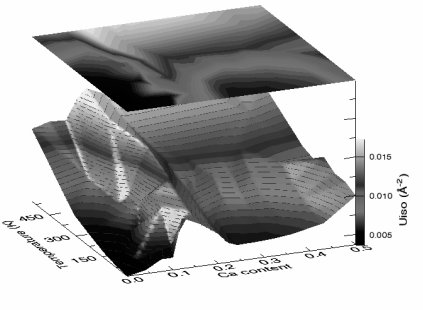

Figure 1. Phase diagram of LCMO CMR manganites mapped out by the isotropic displacement parameter of O2, as obtained from crystallographic modelling using Pbnm space group settings. The ridge centred at around x=0.175 in the 3D plot corresponds to the Jahn-Teller transition.

Typical PDF, G(r), of the x=0 sample is shown in figure 2. The nearest neighbour doublet at ~2 Å corresponds to the 4 shorter and 2 longer Mn-O bonds. The peaks are negative due to

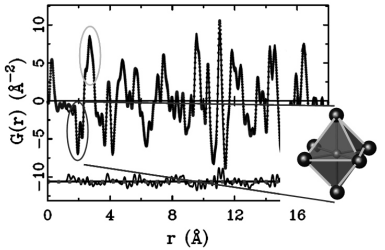

Figure 2. Typical atomic PDF, G(r), of the LCMO system. Symbols represent the data, solid line is the crystallographic model, and the difference curve is offset below. The circled peaks at 2.0 Å and 2.75 Å in PDF correspond to the MnO_6 octahedra locally, to the Mn-O and O-O distances respectively.

the negative neutron scattering length of Mn. Set of positive PDF peaks centred at ~2.75 Å contains O-O bond length contributions. These PDF features, circled in figure 2, capture the local behaviour of the MnO_6 octahedra, and allow systematic tracking of the JT-distortion evolution with temperature and/or doping. New high data throughput neutron powder diffractometers, such as NPDF and GEM, make it feasible to systematically evaluate the local structural behaviour in this manner. In figure 3 (a) and (b) we summarize the results of the evolution of the JT distortion with temperature in x=0 sample, and with doping at 310 K respectively, using the R(r) representation of the PDF. The vertical dashed lines indicate the length of the Mn-O bonds in the ground state of LMO. The dashed profiles denote the O-O' phase transition boundaries in the two cases. There is no appreciable change of the local JT distortion upon crossing into the O' phase, evident in the figures. Moreover, the peaks near

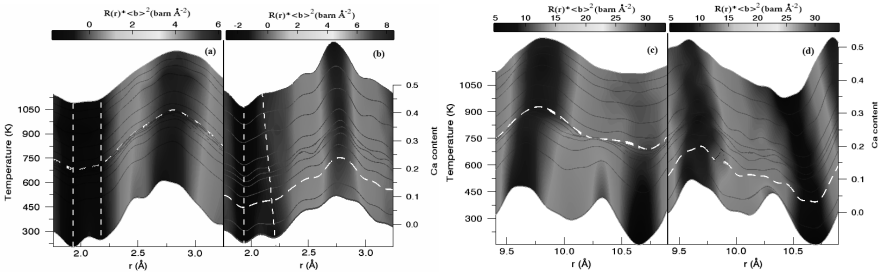

Figure 3. Radial distribution function (RDF), R(r), depicting the evolution of the JT distortion with (a) temperature in the x=0 sample, and with (b) doping at 310K. The vertical dashed lines indicate the positions of the short and long Mn-O bonds in the undoped endmember at 10K. Dashed profiles denote the Jahn-Teller phase boundary. (c) and (d) show the same RDFs with emphasis on the features at slightly higher r-values. Notable is a dramatic change in the 10.3 Å peak across the phase boundary marked with dashed lines.

2.75 Å do not change discontinuously either. The changes that can be noticed are those that are due to the thermal broadening, figure 3 (a), and due to the scattering length change, as Ca doping changes, figure 3 (b). However in both cases the RDF profiles evolve continuously. Rather dramatic change in the local structure is observed around 10.3 Å, figure 3 (c) and (d). There is an abrupt change in this peak intensity on crossing the JT phase line. It has been demonstrated that this effect is related to the rearrangements within the oxygen sublattice [18]. Quantification of these observations, by fitting the PDF profiles over relatively narrow r-range, further showed that the local JT distortion remains unchanged across the Jahn-Teller transition, while the features sensitive to oxygen rotations that correspond to further-neighbour correlations change dramatically and vanish in the pseudo-cubic phase [18].

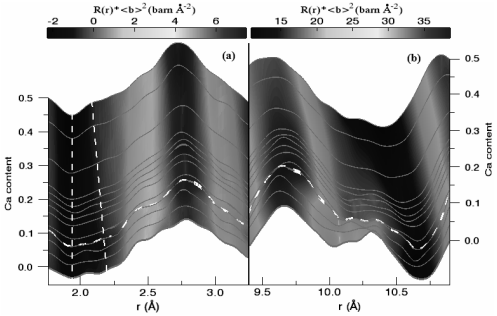

Figure 4. The RDFs of the series of LCMO samples obtained for 550K. All the structural features previously observed as a function of temperature at fixed doping (x=0), and as a function of doping at fixed temperature (T=310K) are reproduced deep in the insulating phase.

Note that there is a systematic gradual shift of the intensity of the 2.17 Å long bond peak towards lower r-values. This, however, continues smoothly across the JT-transition [19].

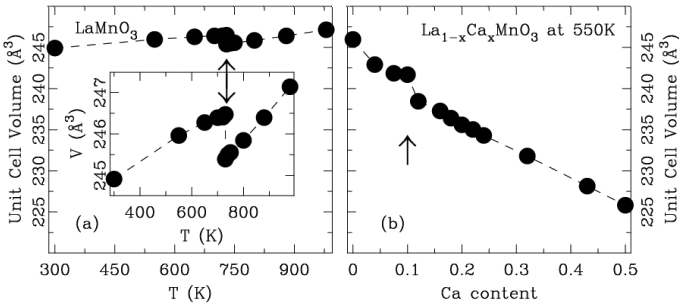

Figure 5. Evolution of the unit cell volume, as obtained from the Rietveld refinement, (a) with temperature at fixed doping (x=0), and (b) with doping at fixed temperature (T=550K). Anomalous unit cell volume reduction is observed at the phase transition (indicated by the arrows) in both cases. Inset to (a) shows the x=0 data in more detail. Dashed lines are guide for the eyes

Figure 4 shows doping evolution at 550 K of the structural features from figure 3. Apart from the apparent shift of the phase boundary towards lower *x*, compared to 310 K, the result is in accord with the earlier findings. In figure 5 (a) the temperature dependence of the crystallographic unit cell volume is shown across the T_{JT}~750 K for x=0 sample, and *on the same scale* in figure 5 (b) the doping dependence of the volume at 550 K across the x_{JT}~0.1. The anomalous volume collapse, presumably due to the repacking of the structure at the transition [14, 16], is observed in both cases. ΔV is estimated to be around 1.1 $Å^3$ (0.41% change across the transition) in the x=0 sample in agreement with earlier results, and about 3.2 $Å^3$ (1.34% change) when the phase boundary is crossed along the doping axis at 550 K. .

Concluding remarks

The neutron powder diffraction based atomic PDF analysis is a powerful tool in accurately tracking the structural evolution of complex materials. The local JT distortion as a function of doping at 550 K persists in the O' phase, while dramatic changes associated with the rearrangement in the oxygen sublattice at T_{JT} are observed. The volume collapse upon crossing into the O' phase along the doping axis at 550 K is observed from the same set of data using Rietveld refinement results. This effect is comparable, but slightly larger than that observed in T-dependence for the x=0 sample.

References

1. Millis, A.J., 1996, *Phys. Rev. B*, **53**, 8483.
2. Ramirez, A.P., 1997, *J. Phys. Condens. Matter*, **9**, 8171.
3. Salamon, M.B. & Jaime, M., 2001, *Rev. Mod. Phys.*, **73**, 583.

4. Milward, G.C., Calderón, M.J. & Littlewood, P.B., 2005, *Nature*, **433**, 607.
5. Dagotto, E., 2005, *Science*, **309**, 257.
6. Schlottmann, P., 2006, *Phys. Rev. B*, **73**, 214428.
7. Wollan, E.O. & Koehler, W.C., 1955, *Phys. Rev.*, **100**, 545.
8. Rodríguez-Carvajal, J., Hennion, M., Moussa, F., Moudden, A. H., Pinsard, L. & Revcolevschi, A., 1998, *Phys. Rev. B*, **57**, R3189.
9. Kim, K.H, Uehara, M., Kiryukhin, V. & Cheong, S.-W., 2002, in *Colossal Magnetoresistive Manganites*, edited by T. Chatterji (Dordrecht: Kluwer–Academic).
10. Tovar, M., Alejandro, G., Butera, A., Caneiro, A., Causa, M.T., Prado, F. & Sánchez, R.D., 1999, *Phys. Rev. B*, **60**, 10199.
11. Zhou, J.-S. & Goodenough, J. B., 1999, *Phys. Rev. B*, **60**, R15002.
12. Zhou, J.-S. & Goodenough, J. B., 2003, *Phys. Rev. B*, **68**, 144406.
13. Mandal, P., Bandyopadhyay, B. & Ghosh, B., 2001, *Phys. Rev. B*, **64**, R180405.
14. Chatterji, T., Fauth, F., Ouladdiaf, B., Mandal, P. & Ghosh, B., 2003, *Phys. Rev. B*, **68**, 052406.
15. Qiu, X., Proffen, Th., Mitchell, J.F. & Billinge, S.J.L., 2005, *Phys. Rev. Lett.*, **94**, 177203.
16. Chatterji, T., Riley, D., Fauth, F., Mandal, P. & Gosh, B., 2006, *Phys. Rev. B*, **73**, 094444.
17. Ahmed, M.R. & Gehring, G.A., 2006, *Phys. Rev. B*, **74**, 014420.
18. Božin, E.S., et al., 2006, *Physica B*, **385**, 110.
19. Božin, E.S., Schmidt, DeConinck, A.J., M., Paglia, G., Mitchell, J.F., Chatterji, T., Radaelli, P.G., Proffen, Th. & Billinge, S.J.L., 2007, *Phys. Rev. Lett.* (in press).
20. Egami, T. & Billinge, S.J.L., 2003, *Underneath the Bragg peaks: structural analysis of complex materials* (Oxford, England: Pergamon Press).
21. Peterson, P.F., Gutmann, M., Proffen, Th. & Billinge, S.J.L., 2000, *J. Appl. Crystallogr.*, **33**, 1192.
22. Proffen, Th. & Billinge, S. J. L., 1999, *J. Appl. Crystallogr.*, **32**, 572.
23. Larson, A.C. & Von Dreele, R.B., 2000, *General Structure Analysis System (GSAS)*, Los Alamos National Laboratory Report LAUR 86-748.
24. Toby, B.H, 2001, *J. Appl. Cryst.*, **34**, 210.

Acknowledgements. This work was supported by the NSF under grant DMR-0304391. Argonne National Laboratory (ANL) is supported by UChicago Argonne, LLC, Operator of ANL. ANL, a U.S. DOE Office of Science laboratory, is operated under Contract No. DE-AC02-06CH11357. This work has benefited from the use of NPDF at the Lujan Center at Los Alamos Neutron Science Center, funded by DOE Office of Basic Energy Sciences. Los Alamos National Laboratory is operated by Los Alamos National Security LLC under DOE Contract DE-AC52-06NA25396.